ACS Medicinal Chemistry Letters
Cite This: ACS Med. Chem. Lett. 2019, 10, 1628−1634
Letter
pubs.acs.org/acsmedchemlett

Structure-Based Design of Selective, Covalent G Protein-Coupled Receptor Kinase 5 Inhibitors

Rachel A. Rowlands,[⊥] M. Claire Cato,[#] Helen V. Waldschmidt,[⊥,∥] Renee A. Bouley,[#] Qiuyan Chen,[▽] Larisa Avramova,[▽] Scott D. Larsen,[⊥] John J. G. Tesmer,[▽] and Andrew D. White*[,⊥]

[⊥]University of Michigan, Vahlteich Medicinal Chemistry Core, College of Pharmacy, 428 Church Street, Ann Arbor, Michigan 48109, United States

[#]University of Michigan, Life Sciences Institute, Departments of Pharmacology and Biological Chemistry, 210 Washtenaw Avenue, Ann Arbor, Michigan 48109, United States

[▽]Purdue University, Departments of Biological Sciences and Medicinal Chemistry and Molecular Pharmacology, 915 W State Street, West Lafayette, Indiana 47907, United States

Supporting Information

ABSTRACT: The ability of G protein-coupled receptor (GPCR) kinases (GRKs) to regulate desensitization of GPCRs has made GRK2 and GRK5 attractive targets for treating heart failure and other diseases such as cancer. Although advances have been made toward developing inhibitors that are selective for GRK2, there have been far fewer reports of GRK5 selective compounds. Herein, we describe the development of GRK5 subfamily selective inhibitors, **5** and **16d** that covalently interact with a nonconserved cysteine (Cys474) unique to this subfamily. Compounds **5** and **16d** feature a highly amenable pyrrolopyrimidine scaffold that affords high nanomolar to low micromolar activity that can be easily modified with Michael acceptors with various reactivities and geometries. Our work thereby establishes a new pathway toward further development of subfamily selective GRK inhibitors and establishes Cys474 as a new and useful covalent handle in GRK5 drug discovery.

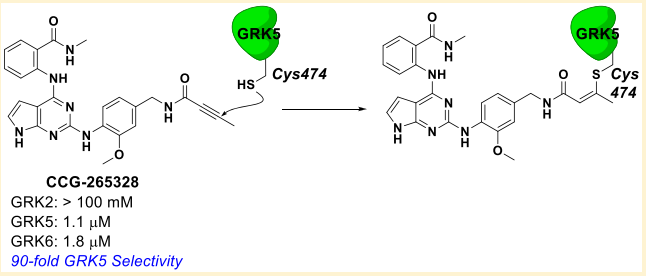

KEYWORDS: *covalent inhibitor, kinase inhibitor, GPCR kinase, heart failure*

Many cellular events are modulated in response to extracellular signals by G protein-coupled receptors (GPCRs).[1] GPCR kinases (GRKs) selectively recognize and phosphorylate activated GPCRs, leading to their desensitization and internalization, which is critical for a normal return to cellular homeostasis.[2] Based on their phylogeny, the seven mammalian GRKs are divided into the GRK1 (GRK1 and 7), GRK2 (GRK2 and 3), and GRK4 (GRK4, 5, and 6) subfamilies.[3] GRK1 and 7 are expressed primarily in the retina and GRK4 in the testes, whereas GRK2, 3, 5, and 6 are more ubiquitously expressed.[4]

Among the GRKs, the β-adrenergic receptor (βAR) kinases (GRK2 and GRK3) are the most widely studied, due to their role in various disease states such as cardiovascular disease, cancer, and inflammation.[5,6] Although GRK5 has been studied for its role in multiple disease states including cancer, neurodegeneration, type 2 diabetes, and cardiovascular disease, few examples of GRK5 selective inhibitors are found in the literature.[7,8] Given its cross-functionality, a selective and potent probe is needed to further investigate the role of GRK5 in the disease states it is implicated in.

Cardiac function is controlled in part by βARs. Under physiological conditions, βARs at the cardiomyocyte cell surface are activated in response to increased circulating levels of the fight-or-flight hormones, epinephrine and norepinephrine, leading to an increase in cardiac output.[9] GRK2 and GRK5, the predominant GRKs expressed in the heart, then regulate signal termination through phosphorylation leading to subsequent internalization of the βARs.[10] In the failing heart, epinephrine and norepinephrine levels remain high in an attempt to compensate for decreased cardiac output.[11] Although initially beneficial for increasing heart contractility, prolonged exposure to catecholamines exacerbates the problem as evidenced by increased GRK2 and GRK5 levels, a decreased number of βARs at the cell surface, and initiation of a pathological hypertrophic stress response.[12] βAR antagonists (β-blockers) are used to treat heart failure, but there is growing evidence that inhibition of GRK2, GRK5, or both could improve the currently available heart failure therapies.[13−20]

There is growing evidence that GRK2 and GRK5 have distinct pathological roles within the failing heart.[21−25] Increased GRK2 levels are thought to mediate the decrease

Received: August 7, 2019
Accepted: November 12, 2019
Published: November 12, 2019

DOI: 10.1021/acsmedchemlett.9b00365
ACS Med. Chem. Lett. 2019, 10, 1628−1634

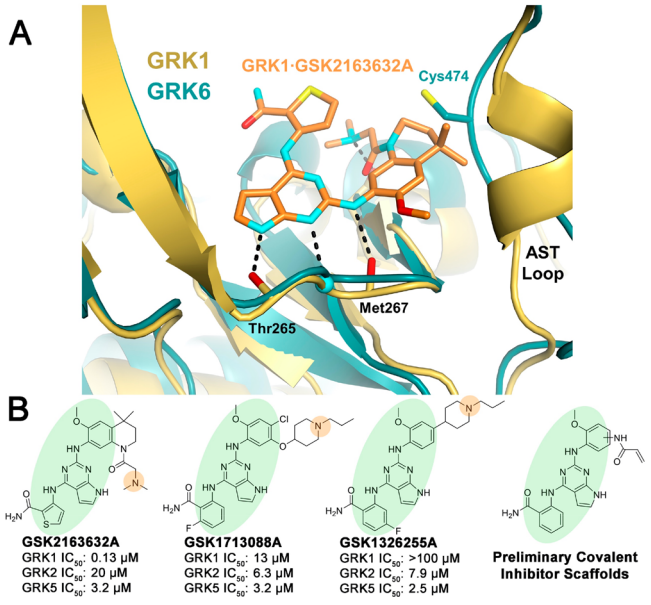

Figure 1. GSK2163632A and related compounds suggest a route to selective inhibition of GRK5 via covalent modification of Cys474. (A) GSK2163632A (green) bound to GRK1 (yellow, PDB entry 4PNI) superimposed with the active conformation of GRK6 (blue, PDB entry 3NYN). (B) Previously identified pyrrolopyrimidine based GRK inhibitors and covalent inhibitor design rationale. Green ovals highlight the base of the scaffold that is generally conserved, and orange circles represent a basic nitrogen that was removed except in the case of analogs where it is replicated potentially by a *N,N*-dimethyl-butenoic amide.

in cell-surface βARs and the prolonged sympathetic nervous system activation, leading to decreased contractility.[22] GRK5 is unique among GRKs in that it undergoes Ca^{2+}·calmodulin-dependent nuclear localization that allows GRK5 to translocate into the nucleus where it phosphorylates histone deacetylase 5, turning on the transcription of hypertrophic genes.[24] Indeed, cardiac-specific GRK2 knockout mice have improved contractility and increased cell-surface βARs postmyocardial infarction,[16] and GRK5 knockout mice are protected from cardiac hypertrophy following controlled cardiac stress. The extent of the functional differences in GRK2 and GRK5 within cardiomyocytes remains to be elucidated, but selective inhibition of each of these kinases would offer the opportunity to further understand their distinct roles in the progression of heart failure. In addition, the selective inhibition of GRK2 or GRK5 presents the possibility of treating different aspects of heart failure without affecting the entire cardiac regulatory system.

Despite high structural similarity in the active site among GRKs, we have had success in developing potent and selective small molecule inhibitors for the GRK2 subfamily that improve contractility in isolated adult mouse cardiomyocytes, in part because GRK2, and presumably GRK3, adopts a distinct inactive pose from other GRKs and other protein kinases.[26−29] Comparison of GRK2 and GRK5 crystal structures revealed a more spacious ATP-binding pocket in GRK2/3 that was able to accommodate bulkier chemical substituents, which allowed us to build out GRK5 binding.[26] We have also developed pan GRK-selective compounds (CCG-215022 and CCG-258748) with nanomolar potency for both GRK2 and GRK5,[26,27,29] but thus far we have not been successful in developing GRK5 selective (or GRK4 subfamily selective) inhibitors using the canonical reversible binding model. Others have reported GRK4 subfamily selective compounds, but they are also potent inhibitors of other kinase families[8] and have not been independently confirmed.

Examination of the crystal structure of GRK6 in what is believed to be an active conformation (PDB 3NYN[30]) revealed that the thiol group of Cys474, located within the flexible active site tether (AST) loop of the kinase domain, is positioned adjacent to the ATP-binding site, at least when the kinase adopts a more closed conformation (Figure 1A). Because this cysteine is unique to GRK4 subfamily members, it could be exploited as a handle for covalent inhibition to gain selectivity for GRK5 over GRK2. In recent years, the popularity of covalent warheads has risen because they offer the possibility of more potency and selectivity than reversible inhibitors.[31] In particular, specifically targeting nonconserved cysteines in the ATP-binding pocket of kinases has demonstrated utility.[31−33] The most successful irreversible modifiers have come from designing a reversibly binding compound with low or sub-μM affinity to also contain a covalent warhead that is within reach and in the proper orientation to interact with the free thiol of a nearby cysteine. The most widely used reaction to achieve irreversible covalent attachment onto a cysteine is a Michael addition using electrophilic warheads such as acrylamides, vinyl sulfones, and alkynes.[33] Recent advances have also been made with the use of an *N,N*-dimethyl-butenoic amide, which improves solubility and contains an internal base that can deprotonate and activate the thiol group.[33−35]

In a previous screen, GSK2163632A was identified as a modestly potent GRK5 inhibitor (IC_{50} = 3.2 μM) with high potency for GRK1 (IC_{50} = 130 nM) and lower potency for PKA (IC_{50} > 500 μM). Two related compounds, GSK1713088A and GSK1326255A (Figure 1B), were shown to have similar potency for GRK5 (IC_{50} = 3.2 and 2.5 μM, respectively), but also modest selectivity over both GRK1 and GRK2.[36] All three GSK compounds share a common pyrrolopyrimidine core, which binds within the ATP pocket with the nitrogens from the core forming hydrogen bonds with the hinge of the kinase domain in a donor−acceptor−donor motif, as observed for GSK2163632A in complex with GRK1 (PDB entry 4PNI, Figure 1A). We therefore hypothesized that we could append covalent warheads to the methoxyphenyl of GSK1713088A or GSK1326255A that could react with Cys474 (Figure 1B). To avoid a highly substituted ring, we replaced the tertiary amine appendages with our covalent warheads in hopes that the potency gained by the covalent bond would overcome the loss of a hydrogen bond accepted by the tertiary amine. The *N,N*-dimethyl-butenoic amide warhead would, however, place a basic tertiary amine in a similar position.

We first rationally designed six different variants of the GSK inhibitor series with short amide linkers. We overlaid a GRK5 crystal structure (PDB entry 4WNK) with that of the active conformation of GRK6 (PDB entry 3NYN) (Figure 1A). Building a covalent warhead *meta* to the aniline (ring C) likely retains the hydrogen bond of the amide carbonyl that GSK2163632A forms with the backbone nitrogen of GRK1-Asp271 (GRK5-Asp270), but this may position the Michael acceptor too distant from Cys474. Alternatively, building the warhead *para* to the aniline would likely hinder the hydrogen bond with Asp271, but may put the Michael acceptor within 1.5 Å of the Cys474 thiol group. However, it is not possible to accurately model these interactions because the degree of

DOI: 10.1021/acsmedchemlett.9b00365
ACS Med. Chem. Lett. 2019, 10, 1628−1634

Table 1. IC_{50} Values for Pyrrolopyrimidine Compounds (μM ± SD)[a]

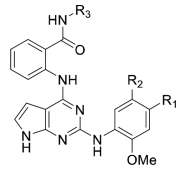

Compound		R_1	R_2	R_3	GRK5 (0 min)	GRK5 (30 min)	GRK5 (60 min)	GRK5 (4 hr)	GRK1 (4 hr)	GRK2 (4 hr)	GRK6 (4 hr)	GRK5 C474S (4 hr)	GRK2/ GRK5[§]
[‡]GSK 2163632A	**1**	NA	NA	H	-	-		3.2	0.13	20	-	-	6.2
[‡]GSK 1713088A	**2**	NA	NA	H	-	-		3.2	13	6.3	-	-	2
[‡]GSK 1326255A	**3**	NA	NA	H	-	-		2.5	> 100	7.9	-	-	3
CCG 262604	**4**		H	H	> 100	> 100	> 100	-	> 100	> 100	-	-	NA
CCG 258903	**5**		H	H	59 ± 90	11.3 ± 5	6.2 ±3	0.22±0.1	> 100	> 100	0.41±0.2	>100	>450
CCG 263045	**6**	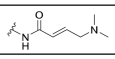	H	H	0.57±0.5	0.30±0.1	0.35±0.1	-	0.76±0.2	0.68±0.03	-	-	2
CCG 262606	**7**	H		H	18 ±10	5.4 ±8	5.9 ±4	>100	> 100	> 100	>100	>100	>17
CCG 258904	**8**	H		H	20 ± 10	6.3 ±4	5.5 ±4	-	>100	39 ±3	-	-	7
CCG 263115	**9**	H	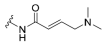	H	0.22±0.03	0.26±0.03	0.27±0.03	-	2.1±0.6	2.7±0.2	-	-	10
CCG 264561	**16a**		H	CH_3	-	-	-	>100	-	>100	>100	>100	NA
CCG 264099	**16b**		H	CH_3	-	-	-	78±20	-	>100	>100	42±40	>1.3
CCG 264629	**16c**	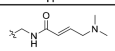	H	CH_3	-	-	-	17±10	-	>100	>100	-	>6
CCG 265328	**16d**		H	CH_3	>100	-	28±20[†]	1.1±0.4	-	>100	1.8±2	0.7±1	>90
CCG 265327	**16e**		H	CH_3	-	-	-	19±20	-	>100	7.7±6	-	>5
CCG 265041	**16f**	H		CH_3	-	-	-	>100	-	2.9±0.6	>100	-	<0.01
CCG 265042	**16g**	H		CH_3	-	-	-	22±5	-	3.2±0.8	18±8	-	0.1
CCG 265044	**16h**	H	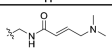	CH_3	-	-	-	4.8±2	-	2.1±2	2.6±2	-	0.4
CCG 265268	**16i**	H		CH_3	-	-	-	>100	-	>100	>100	-	NA
CCG 265267	**16j**	H		CH_3	-	-	-	7.1±3	-	>100	2.5±3	-	>14

[a]Experimental values derived from this report were run three times in duplicate with the exception of assays involving **5** against GRK5, GRK6, and GRK5-C474S with 4 h incubations, which were performed two times in duplicate. Inhibitor incubation times are given in parentheses. [‡]From Homan et al.[38] Note that these compounds were not assayed after 4 h incubations and are listed here for comparison purposes only. [§]Selectivity for GRK5 over GRK2 based on IC_{50} ratio. The IC_{50} value for the longest incubation with GRK5 was used for the calculation. [†]Measured at 100 min.

kinase domain closure and the conformations of the flexible AST and P loops cannot be predicted *a priori*. Therefore, both *para* and *meta* substituents were synthesized, including unreactive saturated ethyl amide analogs as negative controls (Table 1).

Synthesis of *para* analogs **4**, **5**, and **6** (Table 1) and *meta* substituted analogs **7**, **8**, and **9** are described in Schemes S1 and S2, respectively. Tosyl protection of commercially available 4, 6-dichloropyrrolopyrimidine **S1** followed by base-catalyzed aromatic substitution with 2-aminobenzamide gave **S3**.[37] Acid promoted lactam cyclization activated the 2-chloro for substitution with either aniline **S8** or **S12** to give lactams **S4** and **S9**. Hydrolysis using ammonium hydroxide afforded amides **S5** and **S10**. Tosyl deprotection followed by amide coupling provided analogs **4**–**9**.

The *para* and *meta* ethylamide controls, **4** and **7**, respectively, showed substantially different biochemical results indicating a possible structure–activity relationship (SAR) cliff. The *para* substituted ethyl amide **7** showed no activity up to 100 μM against all GRKs tested, whereas **4** showed low micromolar inhibition for GRK5 with an IC_{50} of 5.9 μM. There was no consistent time-dependent change in inhibition of GRK5 by **4** or **7** as a function of time, as expected. The *para* substituted acrylamide, **5**, exhibited an IC_{50} of 6.2 μM for GRK5 after 1 h of preincubation on ice, with no potency against GRK1 or GRK2. After 4 h, **5** showed a convincing increase in potency as a function of time consistent with covalent inhibition, with an IC_{50} of 0.2 μm (Table 1, Figure 2). The >16-fold difference in GRK5 potency for **5** relative to its noncovalent control **4** at 1 h also suggests a covalent

DOI: 10.1021/acsmedchemlett.9b00365
ACS Med. Chem. Lett. 2019, 10, 1628–1634

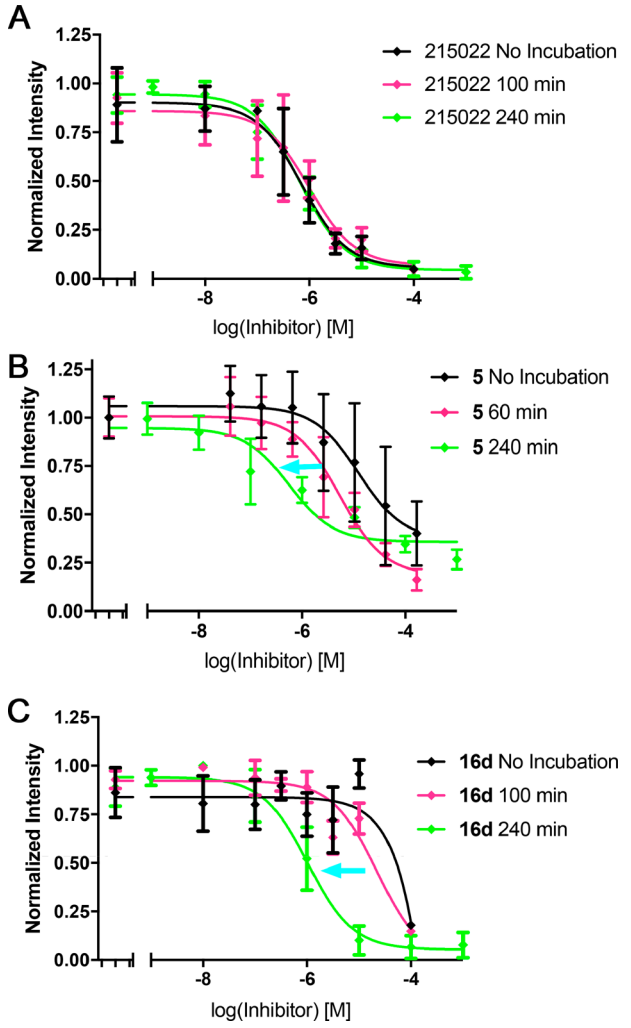

Figure 2. Time-dependent inhibition of GRK5 by **5** and **16d** but not CCG-215022. Compounds were preincubated for times of 0 min (black), 100 min (magenta), and 240 min (green). (A) CCG-215022, which has no covalent modifier, does not show a significant change in IC_{50} (380 nM) over time. Compounds (B) **5** and (C) **16d** exhibit the expected leftward shift in IC_{50} for covalent inhibitors as preincubation times increase, as indicated by the blue arrows. Each curve is the average of either three (215022 and **16d**) or four (**5**) experiments. Error bars represent standard deviation.

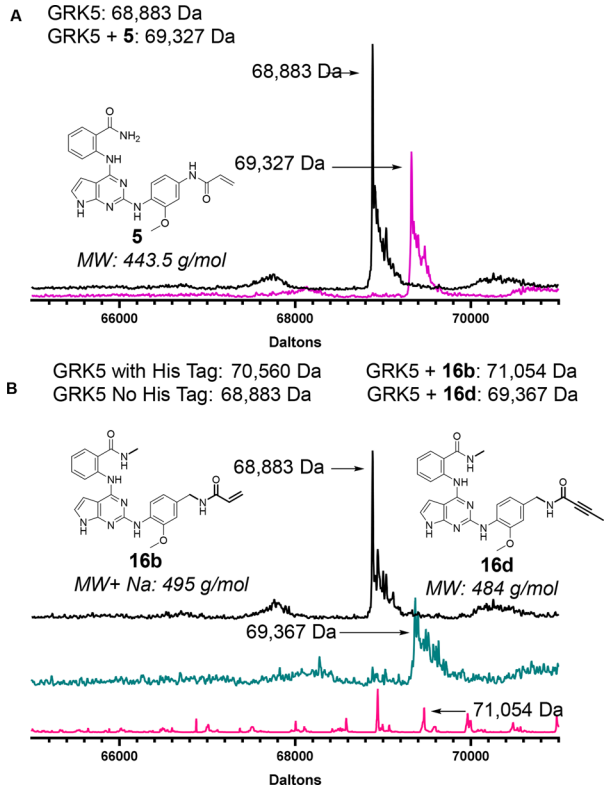

Figure 3. Evidence from intact mass spectrometry for covalent modification of GRK5 by **5**, **16b**, and **16d**: (A) GRK5 only (black trace), GRK5·**5** (purple). (B) MS traces for GRK5 (black trace), GRK5·**16d** (ocean blue), and GRK5·**16b** (pink). The latter trace indicates that **16b** only partially labeled GRK5.

mechanism of action. When **5** was also tested using light activated rod outer segments (ROS) as a substrate instead of tubulin, the inhibitory potency was comparable across all incubation times (Figure S5). This result is consistent with our prior GRK inhibitor studies.[27,38] The compounds also exhibited >450 selectivity over GRK2. The *meta* acrylamide analog **8** had similar potency for GRK5 at all incubation times with respect to its noncovalent control **7** suggesting that it is not acting covalently. It also showed no inhibition of GRK1 but modest GRK2 inhibition (IC_{50} = 39 μM).

Both **6** and **9**, featuring the N,N-dimethyl-butenoic amide in *para* and *meta* positions, respectively, had increased potency for all three GRKs relative to the acrylamide inhibitors **5** and **8**, indicating that addition of the basic nitrogen augments potency against all three kinases. The *para* substituted analog, **6**, was predicted to be closer to the AST loop and thus more likely to form a covalent bond with Cys474. In our time-dependent inhibition of GRK5, it shows some improvement from 0 min to 1 h (GRK5 IC_{50} from 0.57 to 0.35 μM, respectively) but exhibits no selectivity over GRK1 or GRK2 (IC_{50} = 0.76 and 0.68 μM, respectively). The *meta* substituted analog, **9**, did not show time-dependent GRK5 inhibition (IC_{50} range = 0.22−0.27 μM), although it showed ∼10-fold selectivity for GRK5 over GRK1 and GRK2 (IC_{50} = 2.1 and 2.7 μM, respectively). This difference in GRK selectivity between the *meta* and *para* substituted analogs **6** and **9** indicates that the position of the amide linked appendage from the methoxyphenyl ring is one route for gaining GRK5 selectivity. Despite their GRK5 potency, **6** and **9** were not further pursued due to their lack of selectivity against GRK1 and 2.

We next tested whether homologation of the covalent warhead linkers to the methoxyphenyl ring would allow them to better engage Cys474 by adding in an additional rotatable bond. For each series of *para* and *meta* substituted analogs, we expanded our search to test five unique covalent warheads of varying softness (acrylamides through vinyl sulfones; Table 1). In Scheme S3, the benzamide on Ring A was methylated to avoid an acid catalyzed intramolecular ring closure.[37] Synthesis of **16a−j** starts with SEM protection of 4,6-dicholopyrrolopyrimidine (**10**) to give starting material **11**. Compound **11** underwent a base catalyzed aromatic substitution to give **12**. Using a traditional Buchwald−Hartwig cross coupling with 2-methoxy-4-cyanoaniline, compound **13** was achieved. From **13**, the nitrile was reduced using Raney Nickel in methanolic ammonia to give precursor **14**. Using standard amide coupling conditions, compounds **15a−e** were achieved in moderate yields (50−80%). Final compounds **16a−e** were then produced by acid catalyzed SEM deprotection. The *meta*

DOI: 10.1021/acsmedchemlett.9b00365
ACS Med. Chem. Lett. 2019, 10, 1628−1634

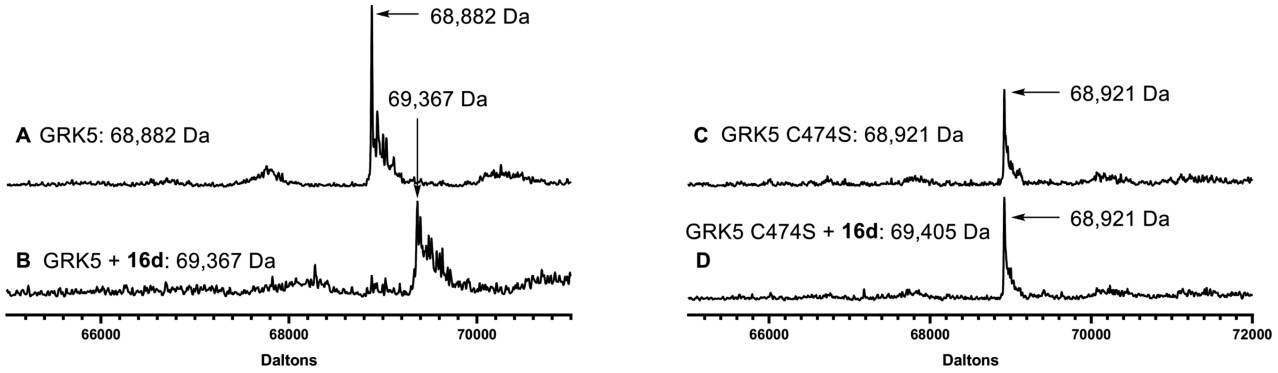

Figure 4. Evidence for GRK5-Cys474 covalent engagement of **16d**. (A) MS trace for GRK5, (B) MS trace for GRK5 incubated with **16d** indicating covalent modification, (C) MS trace for GRK5-C474S, and (D) MS trace for GRK5-C474 incubated with **16d** indicates that **16d** cannot covalently modify GRK5-C474S. Each peak shown is representative of $n = 3$ experiments.

series of compounds **16f–j** were accomplished through a modified route (Scheme S4). Coupling partner **17** was achieved through reduction of the amide (**18**) to the 3-amino-aniline, **19**. Compound **19** was then protected with Cbz-chloride to then yield **17** in 75% yield. Then, using coupling partners **12** and **17**, **13a′** was achieved via a standard Buchwald coupling. Precursor **14a′** was achieved by a reductive Cbz deprotection. From **14a′**, compounds **15f–j** and **16f–j** were furnished using the same coupling and deprotection conditions used in Scheme S4.

We then determined IC_{50} values of the homologated compounds after a 4 h incubation for GRK2, GRK5, and GRK6 (Table 1). GRK6 was included as a positive control for GRK4 subfamily selectivity. As in the nonhomologated series, the ethylamide compounds (**16a** and **16f**) showed an SAR cliff, with the *para* ethylamide unable to inhibit any of the GRKs tested. The reactive *para*-substituted series (**16b–e**) were more selective for GRK5/6 over GRK2 than their *meta* analogs with the exception of **16e**. GRK5 tolerated both the small substituents of the acrylamide **16b** (IC_{50} = 78 μM) and vinyl sulfone, **16e** (IC_{50} = 19 μM), but also the large *N*,*N*-dimethyl-butenoic amide of **16c** (IC_{50} = 17 μM). The *para*-alkyne (**16d**) was the most potent and selective GRK5 inhibitor from this series (IC_{50} = 1.1 μM, 90-fold selectivity over GRK2 after 4 h incubation). Compound **16d** also demonstrated comparable inhibitory potency for GRK5/6 when using light-activated ROS as a substrate instead of tubulin (Figure S5).

Interestingly, potency for GRK2 was lost for all compounds with the *para*-substitution. It is possible that the slightly longer AST-loop in the GRK2 subfamily allows it to reach further in the active site, as seen for residues 476–479 in the GRK2-G$\beta\gamma$·GSK180736A cocrystal structure (PDB entry 4PNK), which would collide with substituents in the *para*-position.

Overall, the *meta* substituted compounds (**16g–j**) tended to have higher potency against GRK5 but lower or even reversed selectivity versus GRK2 (the exception being the vinyl sulfone **16j**). Small polar groups, specifically those with hydrogen bond acceptor capability, were well tolerated in GRK5. For example, both **16g** and **16j** inhibited GRK5, but the polar vinyl sulfone of **16j** was more potent (IC_{50} = 7.1 μM) than the more lipophilic acrylamide of **16g** (IC_{50} = 22 μM). The *meta*-alkyne (**16i**) had no potency for GRK5, suggesting that this more rigid covalent modifier may collide with the P-loop or AST-loop. The **16h** compound had low micromolar potency for GRK5.

Although these compounds selectively inhibit GRK5, they have only modest potency. Our two most potent analogs, **5** and **16d**, have IC_{50} values of 0.22 and 1.1 μM, respectively, after 4 h incubation using tubulin as a substrate (Table 1). We attribute this to one of two reasons. Either the core scaffold has a suboptimal engagement with the hinge region, or the entropic cost of locking down the flexible AST loop via a covalent bond is high enough to limit the binding affinity.

Of the homologated series, only **16g**, **16h**, and **16f** showed activity against GRK2. Our modeling suggested that shorter warheads may be more easily accommodated within the shallow GRK2 ribose pocket. All the other *meta*-substituted materials have larger, less flexible warheads. Our most GRK2 selective analog, **16f**, has only modest potency compared to previously developed GRK2 inhibitors, and we therefore are not pursuing it as a GRK2 lead compound.[26,29]

As expected, inhibition of GRK6 was similar to that of GRK5 in most cases, the exception being **16d**, which was unable to inhibit GRK6. It is unclear whether this represents true intrasubfamily selectivity or a vagary of the experimental conditions for this combination. The most potent compound **16d** was then additionally tested at 0 and 100 min incubations to assess if there was a time-dependent decrease in IC_{50}, the hallmark of covalent inhibition. Indeed, **16d** displayed a marked increase in apparent potency as a function of time (Figure 2). Further confirmation of covalent inhibition of GRK5 was achieved through intact protein mass spectrometry (MS). Compounds **5** and **16a–e** were tested, but only **5**, **16b**, and **16d** showed significant amounts of covalent linkage after a 3 h incubation (Figures 3 and S1), consistent with the results of our radiometric assays. Compounds **16f–j** were also tested but showed no covalent inhibition (Figure S2).

For **5**, **16b**, and **16d**, we also tested whether inhibition is affected when Cys474 is mutated to serine (GRK5-C474S). A decrease in GRK5-C474S potency relative to wild-type GRK5 would thus be consistent with a covalent inhibition mechanism. Compound **5** lost all potency against the mutant protein, whereas **16b** and **16d** retained comparable activity. The reason is unclear, but a structure of GRK5-C474S bound to **16d** would help resolve that discrepancy by illuminating how this particular compound interacts with the Ser474 point mutation.

We next tested whether **16d** engaged GRK5 in a covalent bond specifically at Cys474 using intact protein MS and showed that GRK5-C474S mutant does not react (Figure 4). Using tandem mass spectrometry (MS/MS) we further

DOI: 10.1021/acsmedchemlett.9b00365
ACS Med. Chem. Lett. 2019, 10, 1628–1634

observed that **16d** labels Cys474 but also a cysteine located in a solvent-exposed position in its regulator of G protein signaling homology domain, remote from the active site (Figures S3−S4). This additional labeling event is indicative of a concentration-dependent covalent engagement, and we do not believe that its presence is indicative of a biologically relevant interaction.

In summary, we report what we believe to be the first examples of covalent inhibitors of GRK5, including some that are GRK5 subfamily selective (**5** and **16d**) with high nanomolar to low micromolar potency. We have leveraged the pyrrolopyrimidine scaffold to install *para*-substituted linkers that can interact covalently with the AST from GRK5 but not from GRK2. Additionally, we have shown that Cys474 is selectively targeted by our covalent warheads, validating our design strategy. Moving forward, we aim to further improve the potency of these compounds against GRK5 and GRK6, and to pursue crystal structures of the GRK5/6·**5** and **16d** complexes to confirm their binding poses and the effect of covalent modification on the overall conformation of GRK5. Before examining the effects of our compounds *in vivo* on cardiomyocyte contractility and, ultimately, to parse the role of GRK5 in heart failure, these compounds will also need to be tested for selectivity against other protein kinases.

■ ASSOCIATED CONTENT

Supporting Information

The Supporting Information is available free of charge on the ACS Publications website at DOI: 10.1021/acsmedchemlett.9b00365.

Experimental procedures and supplementary figures (PDF)

■ AUTHOR INFORMATION

Corresponding Author

*Phone: 734-647-7374. E-mail: whitandd@umich.edu.

ORCID

Renee A. Bouley: 0000-0002-1358-0994

Scott D. Larsen: 0000-0001-8440-4990

Andrew D. White: 0000-0001-7869-0118

Present Address

‖(H.V.W.) 130 Scripps Way, Jupiter, FL 33458, USA

Author Contributions

The manuscript was written primarily by R.A.R., M.C.C., and J.G.G.T. All authors have given approval to the final version of the manuscript. H.V.W. synthesized compounds **4**−**9** and determined their IC_{50} values for GRKs 1, 2, and 5. R.A.R. synthesized compounds **16a**−**j** and performed MS experiments. M.C.C. determined IC_{50} values for GRK2, 5, 6, and GRK5-C474S. M.C.C. purified GRK2. R.A.B. purified GRK5, 6, and GRK5-C474S and contributed some of the IC_{50} dose−response experiments. Q.C. and L.A. performed ROS phosphorylation assays.

Funding

This work was supported by NIH grants HL071818 and HL122416 and the Walther Cancer Foundation (to J.J.G.T.), American Heart Association grants 15PRE22730028 (to H.V.W.) and 19POST3445019 (to Q.C.), and a pilot grant from the University of Michigan Center for Discovery of New Medicines (to A.D.W.). M.C.C. acknowledges training grant support from the University of Michigan Chemistry−Biology Interface (CBI) training program (NIH grant 5T32GM008597).

Notes

The authors declare no competing financial interest.

■ ACKNOWLEDGMENTS

We thank Dr. Venky Bashar of the University of Michigan Proteomic Resource Facility for assistance with tandem mass spectrometry efforts. We also thank Dr. Pil Lee for her technical assistance in building a GRK5 homology model.

■ ABBREVIATIONS

GPCR, G protein-coupled receptor; GRK, G protein-coupled receptor kinase; βAR, β-adrenergic receptor; AST, active site tether; P-loop, phosphate-binding loop; MS, mass spectrometry

■ REFERENCES

(1) Katritch, V.; Cherezov, V.; Stevens, R. C. Structure-Function of the G Protein−Coupled Receptor Superfamily. *Annu. Rev. Pharmacol. Toxicol.* **2013**, *53* (1), 531−556.

(2) Gurevich, E. V.; Tesmer, J. J. G.; Mushegian, A.; Gurevich, V. V. G. Protein-Coupled Receptor Kinases: More than Just Kinases and Not Only for GPCRs. *Pharmacol. Ther.* **2012**, *133* (1), 40−69.

(3) Pitcher, J. A.; Freedman, N. J.; Lefkowitz, R. J. G. Protein-Coupled Receptor Kinases. *Annu. Rev. Biochem.* **1998**, *67* (1), 653−692.

(4) Ferguson, S. S. Evolving Concepts in G Protein-Coupled Receptor Endocytosis: The Role in Receptor Desensitization and Signaling. *Pharmacol. Rev.* **2001**, *53* (1), 1−24.

(5) Nogués, L.; Palacios-García, J.; Reglero, C.; Rivas, V.; Neves, M.; Ribas, C.; Penela, P.; Mayor, F. G. Protein-Coupled Receptor Kinases (GRKs) in Tumorigenesis and Cancer Progression: GPCR Regulators and Signaling Hubs. *Semin. Cancer Biol.* **2018**, *48*, 78−90.

(6) Steury, M. D.; McCabe, L. R.; Parameswaran, N. G. Protein-Coupled Receptor Kinases in the Inflammatory Response and Signaling. *Adv. Immunol.* **2017**, *136*, 227−277.

(7) Hendrickx, J. O.; van Gastel, J.; Leysen, H.; Santos-Otte, P.; Premont, R. T.; Martin, B.; Maudsley, S. GRK5 − A Functional Bridge Between Cardiovascular and Neurodegenerative Disorders. *Front. Pharmacol.* **2018**, *9*, 04184.

(8) Cho, S. Y.; Lee, B. H.; Jung, H.; Yun, C. S.; Ha, J. D.; Kim, H. R.; Chae, C. H.; Lee, J. H.; Seo, H. W.; Oh, K.-S. Design and Synthesis of Novel 3-(Benzo[d]Oxazol-2-Yl)-5-(1-(Piperidin-4-Yl)-1H-Pyrazol-4-Yl)Pyridin-2-Amine Derivatives as Selective G-Protein-Coupled Receptor Kinase-2 and −5 Inhibitors. *Bioorg. Med. Chem. Lett.* **2013**, *23* (24), 6711−6716.

(9) Huang, Z. M.; Gold, J. I.; Koch, W. J. G. Protein-Coupled Receptor Kinases in Normal and Failing Myocardium. *Front. Biosci., Landmark Ed.* **2011**, *16* (1), 3057−3060.

(10) Lohse, M. J.; Engelhardt, S.; Eschenhagen, T. What Is the Role of β-Adrenergic Signaling in Heart Failure? *Circ. Res.* **2003**, *93*, 896−906.

(11) Triposkiadis, F.; Karayannis, G.; Giamouzis, G.; Skoularigis, J.; Louridas, G.; Butler, J. The Sympathetic Nervous System in Heart Failure. *J. Am. Coll. Cardiol.* **2009**, *54* (19), 1747−1762.

(12) Port, J. D.; Bristow, M. R. Altered Beta-Adrenergic Receptor Gene Regulation and Signaling in Chronic Heart Failure. *J. Mol. Cell. Cardiol.* **2001**, *33* (5), 887−905.

(13) Rockman, H. A.; Chien, K. R.; Choi, D.-J.; Iaccarino, G.; Hunter, J. J.; Ross, J.; Lefkowitz, R. J.; Koch, W. J. Expression of a -Adrenergic Receptor Kinase 1 Inhibitor Prevents the Development of Myocardial Failure in Gene-Targeted Mice. *Proc. Natl. Acad. Sci. U. S. A.* **1998**, *95* (12), 7000−7005.

(14) Eckhart, A. D.; Ozaki, T.; Tevaearai, H.; Rockman, H. A.; Koch, W. J. Vascular-Targeted Overexpression of G Protein-Coupled Receptor Kinase-2 in Transgenic Mice Attenuates Beta-Adrenergic

DOI: 10.1021/acsmedchemlett.9b00365
ACS Med. Chem. Lett. 2019, 10, 1628−1634

Receptor Signaling and Increases Resting Blood Pressure. *Mol. Pharmacol.* **2002**, *61* (4), 749−758.
(15) Kohout, T. A. Regulation of G Protein-Coupled Receptor Kinases and Arrestins During Receptor Desensitization. *Mol. Pharmacol.* **2003**, *63* (1), 9−18.
(16) Raake, P. W.; Vinge, L. E.; Gao, E.; Boucher, M.; Rengo, G.; Chen, X.; DeGeorge, B. R.; Matkovich, S.; Houser, S. R.; Most, P.; et al. Protein−Coupled Receptor Kinase 2 Ablation in Cardiac Myocytes Before or After Myocardial Infarction Prevents Heart Failure. *Circ. Res.* **2008**, *103* (4), 413−422.
(17) Thal, D. M.; Homan, K. T.; Chen, J.; Wu, E. K.; Hinkle, P. M.; Huang, Z. M.; Chuprun, J. K.; Song, J.; Gao, E.; Cheung, J. Y.; et al. Paroxetine Is a Direct Inhibitor of G Protein-Coupled Receptor Kinase 2 and Increases Myocardial Contractility. *ACS Chem. Biol.* **2012**, *7* (11), 1830−1839.
(18) Lymperopoulos, A.; Rengo, G.; J. Koch, W. GRK2 Inhibition in Heart Failure: Something Old, Something New. *Curr. Pharm. Des.* **2012**, *18* (2), 186−191.
(19) Raake, P. W. J.; Schlegel, P.; Ksienzyk, J.; Reinkober, J.; Barthelmes, J.; Schinkel, S.; Pleger, S.; Mier, W.; Haberkorn, U.; Koch, W. J.; et al. AAV6.BARKct Cardiac Gene Therapy Ameliorates Cardiac Function and Normalizes the Catecholaminergic Axis in a Clinically Relevant Large Animal Heart Failure Model. *Eur. Heart J.* **2013**, *34*, 1437−1447.
(20) Cannavo, A.; Liccardo, D.; Koch, W. J. Targeting Cardiac β-Adrenergic Signaling via GRK2 Inhibition for Heart Failure Therapy. *Front. Physiol.* **2013**, *4*, 1−7.
(21) Penela, P.; Murga, C.; Ribas, C.; Tutor, A.; Peregrin, S.; Mayorjr, F. Mechanisms of Regulation of G Protein-Coupled Receptor Kinases (GRKs) and Cardiovascular Disease. *Cardiovasc. Res.* **2006**, *69* (1), 46−56.
(22) Lymperopoulos, A.; Rengo, G.; Funakoshi, H.; Eckhart, A. D.; Koch, W. J. Adrenal GRK2 Upregulation Mediates Sympathetic Overdrive in Heart Failure. *Nat. Med.* **2007**, *13* (3), 315−323.
(23) Kemp, C. D.; Conte, J. V. The Pathophysiology of Heart Failure. *Cardiovasc. Pathol.* **2012**, *21* (5), 365−371.
(24) Traynham, C. J.; Hullmann, J.; Koch, W. J. Canonical and Non-Canonical Actions of GRK5 in the Heart. *J. Mol. Cell. Cardiol.* **2016**, *92*, 196−202.
(25) Hullmann, J.; Traynham, C. J.; Coleman, R. C.; Koch, W. J. The Expanding GRK Interactome: Implications in Cardiovascular Disease and Potential for Therapeutic Development. *Pharmacol. Res.* **2016**, *110*, 52−64.
(26) Waldschmidt, H. V.; Homan, K. T.; Cruz-Rodríguez, O.; Cato, M. C.; Waninger-Saroni, J.; Larimore, K. M.; Cannavo, A.; Song, J.; Cheung, J. Y.; Kirchhoff, P. D.; et al. Structure-Based Design, Synthesis, and Biological Evaluation of Highly Selective and Potent G Protein-Coupled Receptor Kinase 2 Inhibitors. *J. Med. Chem.* **2016**, *59* (8), 3793−3807.
(27) Waldschmidt, H. V.; Homan, K. T.; Cato, M. C.; Cruz-Rodríguez, O.; Cannavo, A.; Wilson, M. W.; Song, J.; Cheung, J. Y.; Koch, W. J.; Tesmer, J. J. G.; et al. Structure-Based Design of Highly Selective and Potent G Protein-Coupled Receptor Kinase 2 Inhibitors Based on Paroxetine. *J. Med. Chem.* **2017**, *60* (7), 3052−3069.
(28) Yao, X.-Q.; Cato, M. C.; Labudde, E.; Beyett, T. S.; Tesmer, J. J. G.; Grant, B. J. Navigating the Conformational Landscape of G Protein−Coupled Receptor Kinases during Allosteric Activation. *J. Biol. Chem.* **2017**, *292* (39), 16032−16043.
(29) Bouley, R.; Waldschmidt, H. V.; Cato, M. C.; Cannavo, A.; Song, J.; Cheung, J. Y.; Yao, X.-Q.; Koch, W. J.; Larsen, S. D.; Tesmer, J. J. G. Structural Determinants Influencing the Potency and Selectivity of Indazole-Paroxetine Hybrid G Protein−Coupled Receptor Kinase 2 Inhibitors. *Mol. Pharmacol.* **2017**, *92* (6), 707−717.
(30) Boguth, C. A.; Singh, P.; Huang, C.; Tesmer, J. J. G. Molecular Basis for Activation of G Protein-Coupled Receptor Kinases. *EMBO J.* **2010**, *29* (19), 3249−3259.
(31) Singh, J.; Petter, R. C.; Baillie, T. A.; Whitty, A. The Resurgence of Covalent Drugs. *Nat. Rev. Drug Discovery* **2011**, *10* (4), 307−317.
(32) Leproult, E.; Barluenga, S.; Moras, D.; Wurtz, J.-M.; Winssinger, N. Cysteine Mapping in Conformationally Distinct Kinase Nucleotide Binding Sites: Application to the Design of Selective Covalent Inhibitors. *J. Med. Chem.* **2011**, *54* (5), 1347−1355.
(33) Liu, Q.; Sabnis, Y.; Zhao, Z.; Zhang, T.; Buhrlage, S. J.; Jones, L. H.; Gray, N. S. Developing Irreversible Inhibitors of the Protein Kinase Cysteinome. *Chem. Biol.* **2013**, *20* (2), 146−159.
(34) Zhang, T.; Inesta-Vaquera, F.; Niepel, M.; Zhang, J.; Ficarro, S. B.; Machleidt, T.; Xie, T.; Marto, J. A.; Kim, N.; Sim, T.; et al. Discovery of Potent and Selective Covalent Inhibitors of JNK. *Chem. Biol.* **2012**, *19* (1), 140−154.
(35) Keating, G. M. Afatinib: A Review of Its Use in the Treatment of Advanced Non-Small Cell Lung Cancer. *Drugs* **2014**, *74* (2), 207−221.
(36) Homan, K. T.; Larimore, K. M.; Elkins, J. M.; Szklarz, M.; Knapp, S.; Tesmer, J. J. G. Identification and Structure−Function Analysis of Subfamily Selective G Protein-Coupled Receptor Kinase Inhibitors. *ACS Chem. Biol.* **2015**, *10* (1), 310−319.
(37) Stevens, K.; Shotwell, J. B.; Redman, A.; Wilson, J. W.; Lei, H.; Gerding, R.; Patnaik, S. Pyrrolopyrimidine Compounds. WO 2010045451 A1, April 22, 2010.
(38) Homan, K. T.; Wu, E.; Wilson, M. W.; Singh, P.; Larsen, S. D.; Tesmer, J. J. G. Structural and Functional Analysis of G Protein−Coupled Receptor Kinase Inhibition by Paroxetine and a Rationally Designed Analog. *Mol. Pharmacol.* **2014**, *85* (2), 237−248.

DOI: 10.1021/acsmedchemlett.9b00365
ACS Med. Chem. Lett. 2019, 10, 1628−1634